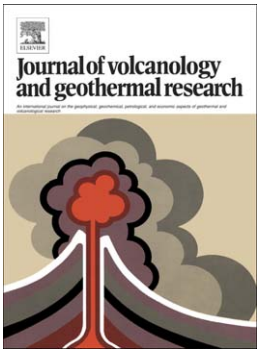

Modeling magmatic accumulations in the upper crust: Metamorphic implications for the country rock

Madison M. Douglas, Adelina Geyer, Antonio M. Álvarez-Valero, Joan Martí

PII: S0377-0273(16)30018-X
DOI: doi: 10.1016/j.jvolgeores.2016.03.008
Reference: VOLGEO 5788

To appear in: *Journal of Volcanology and Geothermal Research*

Received date: 23 October 2015
Revised date: 29 February 2016
Accepted date: 8 March 2016

Please cite this article as: Douglas, Madison M., Geyer, Adelina, Álvarez-Valero, Antonio M., Martí, Joan, Modeling magmatic accumulations in the upper crust: Metamorphic implications for the country rock, *Journal of Volcanology and Geothermal Research* (2016), doi: 10.1016/j.jvolgeores.2016.03.008

Modeling magmatic accumulations in the upper crust: metamorphic implications for the country rock

Madison M. Douglas[1], Adelina Geyer[2], Antonio M. Álvarez-Valero[3], Joan Martí[2]

[1] *Department of Earth, Atmospheric and Planetary Sciences, Massachusetts Institute of Technology, Cambridge, Massachusetts, USA*

[2] *Group of Volcanology, SIMGEO (UB-CSIC), Institute of Earth Sciences Jaume Almera, ICTJA-CSIC, Lluis Solé i Sabaris s/n, 08028 Barcelona, Spain*

[3] *Department of Geology, University of Salamanca, Spain*

Corresponding author: Adelina Geyer, Group of Volcanology, SIMGEO (UB-CSIC), Institute of Earth Sciences Jaume Almera, ICTJA-CSIC, Lluis Solé i Sabaris s/n, 08028 Barcelona, Spain. (ageyer@ictja.csic.es)

Abstract

Field exposures of magma chambers tend to reveal contact metamorphic aureoles in the surrounding crust, which width varies from few centimeters to kilometers. The igneous accumulation not only increases the temperature around it, but also weaks its surrounding country rock beyond the brittle-ductile transition temperature. The formation of a ductile halo around the magmatic reservoir may significantly impact into the stability and growth of the magma chamber, as well as into potential dyke injections and processes of ground deformation. In this paper, we examine how a magmatic accumulation affects the country

rock through the combination of petrologic and thermal perspectives. For this, we numerically modelled (i) the conductive cooling of an instantaneously emplaced magma chamber within compositionally representative pelitic and carbonate upper crusts, and (ii) the corresponding changes in the viscosity of the host rock potentially leading to ductile regimes. We consider basaltic to rhyolitic magma chambers at different depths with oblate, prolate and spherical geometries. The resulting temperature field distribution at different time steps is integrated with crustal metamorphic effects through phase diagram modeling. Our results indicate that the geometry of the magma accumulations play a dominant role in controlling the local metamorphic and thermal effects on the country rocks. They conclude that (i) the combination of relatively simple geothermal models with petrologic datasets can generate first order predictions for the maximum metamorphic grade and geometry of magma chamber aureoles; (ii) the possible changes in the mechanical properties of the country rock are not necessarily linked to the petrological changes in contact aureoles; and (iii) the present rheologic outcomes may be used in further studies of magma chamber stability and integrity, which may favor the understanding of the melt transfer throughout the crust.

Keywords

Thermal effects, magma chamber, upper crust, contact metamorphism, numerical simulation, equilibrium mineral assemblage

1. Introduction

The past few decades have been marked by an important investigation into quantifying the thermal effects of igneous accumulations on the surrounding host rock (e.g. Lovering, 1935; 1936; 1955;Jaeger, 1959;Carrigan, 1983; 1988;Cui et al., 2001;Wang et al., 2012;Pla and Álvarez-Valero, 2015). This effort is crucial to understanding and evaluating related phenomena, such as contact metamorphism processes (e.g. Cook and Bowman, 1994;Cui et al., 2001;Annen et al., 2006;Bufe et al., 2014) and the maturation of organic matter in the vicinity of magma reservoirs (e.g. Galushkin, 1997;Fjeldskaar et al., 2008). The correlation between the results of mathematical models and geothermometers, such as vitrinite reflectance and fluid inclusions (Galushkin, 1997;Wang, 2012 and references therein), has widely demonstrated the capability of these studies to reconstruct the thermal evolution of host rocks after an igneous accumulation.

Numerous petrological observations and numerical simulations indicate that crustal aureoles due to contact metamorphism encompass a variety of widths, ranging from few centimeters to some kilometers (e.g. Bowers et al., 1990;Johnson et al., 2011;Peacock and Spear, 2013;Bufe et al., 2014). The extent and degree of the generated aureole depend on many parameters, including: temperature, composition and thermal properties (i.e. thermal conductivity, specific heat capacity) of the magma and country rock; the degree of crystallization of the magma; the size and geometry of the reservoir; the latent heat of fusion for the crystallizing magma; and the amount of heat energy consumed by endothermic metamorphic reactions taking place in the aureole (Johnson et

al., 2011;Peacock and Spear, 2013). Additionally, at shallow crustal levels, hydrothermal processes may play an important role in incorporating cations and H_2O into the system, as well as redistributing the heat released from the cooling magma reservoir that can affect contact metamorphism equilibria (e.g. Peacock and Spear, 2013).

In parallel to the work focused on the mineralogical and petrological consequences of igneous accumulations, several studies have attempted to elucidate and quantify their effects on the country rock. For instance, the mathematical models by Dragoni and Magnanensi (1989), Jellinek and DePaolo (2003), Del Negro et al. (2009) and Gregg et al. (2013) revealed changes in the host rock's rheology due to the thermal effects of the cooling magma reservoir. Other authors indicated these changes in the country rock rheology may influence magma chamber growth, rupture (i.e. dike intrusion), or even caldera collapse events (Jellinek and De Paolo, 2003; Gregg et al., 2012, 2013; Gottsmann and Odbert, 2014). Indeed, recent works by Gregg and coauthors (2012, 2013) define the thermal alteration of the host rock to be a key parameter controlling the dynamics and genesis of caldera-forming eruptions of giant magmatic reservoirs. The temperature increase of the country rock translates into a considerably decrease of its viscosity and Young's modulus, causing host rock rheology to switch from brittle to ductile (Gregg et al., 2012). Depending on the size and shape of the magma reservoir, as well as on new magma influx, the "ductile aureole" formed around the magma chamber then inhibits potential dike injections into the surrounding rock, creating positive feedback in the magma accumulation process by increasing the chamber's stability and growth rate (Jellinek and De Paolo, 2003;Gregg et al., 2012, 2013). Hence, if no dykes are injected, when more magma arrives into the reservoir, its volume increases, along

with corresponding thermal effects on the country rock. This process favors the survival and growth of the thermal aureole.

Traditionally, the thermal alteration of both the mechanical properties and petrological features of the host rock due to magmatic accumulations have been treated separately (e.g. Dragoni and Magnanensi, 1989;Cui et al., 2001;Gottsmann and Odbert, 2014). However, assumptions of the geometries, temperature distributions, and rheology in the plumbing system of the magma chamber require input from petrological studies. Likewise, the complete interpretation of any petrological dataset requires key numerical parameters constrained by magma chamber rheology (e.g. Álvarez-Valero et al., 2015).

The final objective of the present research is to understand the metamorphic signatures of different magmatic reservoirs in the host rock and to examine whether or not these are related to particular changes in its mechanical properties. We aim to link the petrological changes observable in the field—as mineral equilibria of contact metamorphism—to possible variations in the country rock viscosity, and vice versa. Does the country rock always undergo a potential transition in its rheology (from brittle to ductile)? If so, is this systematically associated with certain petrological changes?

For this, we carry out a series of heat transfer models of the conductive cooling of different instantaneously emplaced magma chambers in three representative pelitic and carbonate upper crusts. For the cooling models, we solve the conductive heat transfer equation using the Finite Element Method (FEM) in an axisymmetric medium. We examine magma chambers of rhyolitic, andesitic, and basaltic composition in oblate, prolate, and spherical reservoirs. Using the modeled temperature field distribution in the host rock through time, we estimate its change in viscosity due to the temperature increase. Finally, we predict the equilibrium mineral assemblage by overlaying the

corresponding phases from pressure-temperature (P-T) pseudosections of the representative crustal bulk compositions.

2. Methodology

2. 1 **Heat transfer models**

The temperature distribution within the magma chamber and the host rock is calculated using FEM, by solving the pure conductive heat transfer equation, and assuming the effects of viscous heating and pressure-volume work are negligible (see Rodríguez et al., 2015 for further details):

$$\rho\, Cp\, \frac{\partial T}{\partial t} + \nabla(-k\nabla T) = \boldsymbol{Q} \qquad \textbf{[1]}$$

where the equation parameters refer to density (ρ), specific heat capacity at constant pressure (Cp), temperature (T), time (t), thermal conductivity (k) and $\boldsymbol{Q}$ denotes heat sources other than viscous heating (see Table 1 for details of the thermal and physical parameters).

Symbol	Value	Variable	SI Unit
A_D	10^9	Dorn parameter	Pa s
Cp		Specific heat capacity at constant pressure	J/(kg K)
Cp_{crust}	Supp. Mat. Table S8	Specific heat capacity of crust[4]	J/(kg K)
Cp_{melt}	Supp. Mat. Tables S4-6	Specific heat capacity of magma (melt phase)	J/(kg K)
Cp_{solid}	Supp. Mat. Tables S4-6	Specific heat capacity of magma (solid phase)	J/(kg K)
d	Supp. Mat. Table S7	Magma chamber depth	km
e	0.25-2	Magma chamber aspect ratio	-
E_A	120,000	Activation energy	J/mol
h	1.061-9.141	Magma chamber height	km
κ_{magma}		Thermal diffusivity of magma [4]	m^2/s
κ_{crust}	Supp. Mat. Table S8	Thermal diffusivity of crust[4]	m^2/s
k	$\rho \cdot Cp \cdot \kappa$	Thermal conductivity	W/(m K)
L	400	Latent heat of crystallization[1]	kJ/kg
θ	Supp. Mat. Tables S1-3	Melt fraction[3]	-
Q_{mantle}	0.03	Subcrustal heat flow[1]	W/m^2
$Q_{surface}$	0.07	Surface heat flow[1]	W/m^2
ρ_{crust}	2700	Crust density	kg/m^3
ρ_{magma}	2344-2694	Magma density[3]	kg/m^3
ϕ	1- θ	Solid fraction[3]	-
R	8.314	Molar gas constant	J/(mol K)
thermal_grad	25-30	Crustal thermal gradient	K/km
T_liquidus	Supp. Mat. Tables S1-3	Magma liquidus temperature[3]	K
T_solidus	Supp. Mat. Tables S1-3	Magma solidus temperature[3]	K
T_surface	298.15	Surface temperature	K
T_{0_magma}		Initial magma temperature	K
T_{0_crust}		Initial crustal temperature	K
P	$1\text{-}3\times10^6$	Magma chamber internal pressure at $h/2$	Pa
ν	Eq. 3	Country rock viscosity	Pa s
w	4.243-19.696	Magma chamber width	km

1, Bea (2010); 2, Whittington et al. (2009); 3, use Rhyolite MELTS code by Gualda et al. (2012); 4 Rodríguez et al. (2015)

Table 1: Physical and thermal parameters

We consider the modeled magma chamber to be emplaced immediately before it begins cooling. The completely liquefied magma reservoir (Gelman et al., 2013) is assumed to intrude in a single episode without further replenishment (Gutiérrez and Parada, 2010). The geometric modeling, mesh discretization and numerical computations are carried out with COMSOL Multiphysics v4.4 software package (http://www.comsol.com). To simulate the solidifying magma, we use the *heat transfer with phase change* module, which allows us to solve Equation 1 after setting the properties of a phase-change material (from liquid to solid) according to the Apparent Heat Capacity formulation (AHC) (see Rodríguez et al., 2015 and references therein). The AHC formulation is considered to be the best representation of a naturally occurring wide phase-change temperature interval, as occurs during magma cooling (Rodríguez et al., 2015). The latent heat of crystallization is accounted for by increasing the heat capacity of the material within the phase change temperature range. For further details on the methodology, the reader is referred to the work by Rodríguez et al. (2015). A comprehensive report detailing one of the models, which includes all settings within COMSOL (e.g. model properties; physics settings; geometry; mesh), as well as an example of one of the models, are available from the corresponding author upon request (COMSOL Multiphysics commercial software V4.4 or greater and *heat transfer with phase change* module are required).

The performed FE models are axisymmetric and constructed over a cylindrical coordinate system with positive *z* values related to altitudes above sea level (Fig. 1a). The magma chamber geometry is oblate, spherical or prolate in shape with height *h* and width *w* (Fig. 1a). The computational domain corresponds to a section of the crust with a 40 km

radius stretching to a depth of 40 km below sea level (Fig. 1a). The FE mesh consists of between 200,000 and 400,000 linear triangular elements up to 250 m in size farther from the magma reservoir, and 2 m in size near the edge of the magma chamber (Fig. 1b). Time steps taken to perform the calculations range from less than a year at the beginning of the cooling processes, up to 300 years to speed calculations once reached the metamorphic peak. We have tested that the chosen time steps do not affect the results obtained.

The selected starting magmatic compositions for the numerical simulations correspond to three representative types that range from alkaline basalt to rhyolite (Table 2). The former, typical of intraplate magmatism, is taken from Polat (2009). The intermediate magma is of andesitic composition and from a subduction zone taken from Yogodzinski et al. (1994). The rhyolitic composition is from an archetypal case of pelitic crustal melting taken from Sensarna et al. (2004). Depending on the model, pressure at the magma chamber center ranges from 1 to 3 kbar (Supplementary Material, Table S1).

Major elements (wt%)	Andesite 35-10/3 [1]	Rhyolite DM 4 [2]	Alkaline Basalt SC95-86 [3]
SiO_2	56.88	75	50
TiO_2	0.68	0.29	2.2
Al_2O_3	18.36	11.69	13.5
FeO*	4.72	2.8	13.95
MgO	4.04	0.15	4.9
MnO	0.1	0.03	0.3
CaO	7.48	0.79	9.6
Na_2O	4.05	2.2	3.2
K_2O	1.3	5.11	0.4
P_2O_5	0.11	0.04	0.4

* FeO as total iron

[1] Yogodzinski et al., 1994

[2] Sensarma et al., 2004

[3] Polat, 2009

Table 2: Starting magma compositions for the different numerical simulations

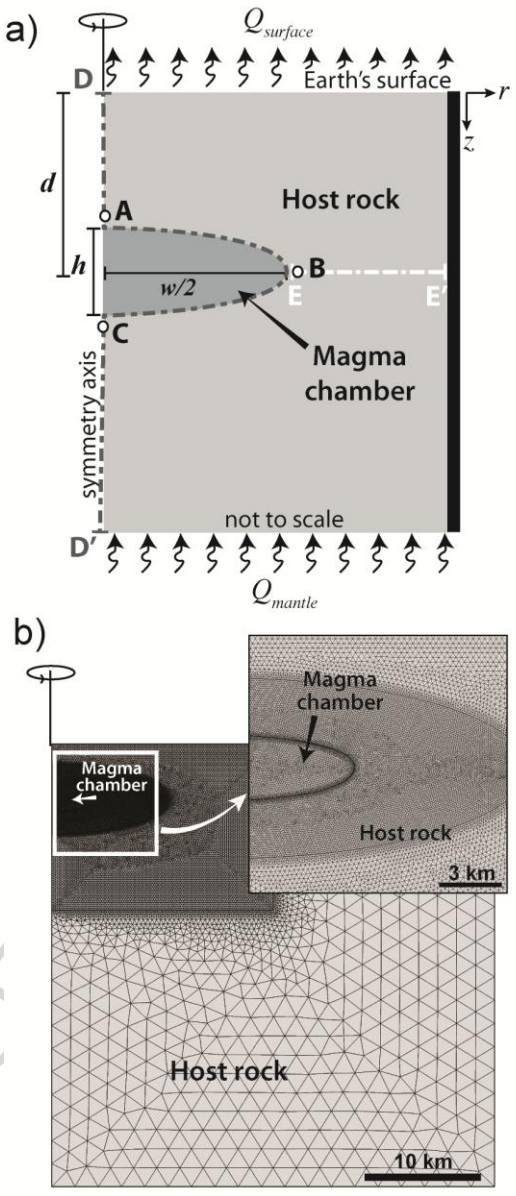

Figure 1 (single column): *(a) Sketch of the numerical model set-up, with applied boundary conditions indicated. (b) Example of the Finite Element mesh used for modeling runs. See Table 1 and the text for further explanation of the different parameters.*

The melt (θ) and solid (ϕ) fractions, as well as the thermal properties of the crystallizing magmas, are determined using the Rhyolite-MELTS code (Gualda et al., 2012). Results are reported in the Supplementary Material (Table S2 – S7) and are used as input data for the models. We simulate isobaric cooling at 1, 2 and 3 kbar pressure, with redox conditions one log unit above the quartz-fayalite-magnetite (QFM) oxygen buffer.

Using the thermal properties provided by MELTS, we explicitly account for the temperature dependence of thermal diffusivity (κ) and heat capacity (C_P). Incorporating a temperature-dependent diffusivity is critical due to its strong influence on the temperature-dependence of thermal conductivity ($k = \rho \cdot C_P \cdot \kappa$) at high temperatures (Nabelek et al., 2012). Average magma density ρ_{magma} values obtained from MELTS are 2344 kg/m^3, 2440 kg/m^3 and 2694kg/m^3 for the rhyolitic, andesitic and basaltic magmas, respectively. For most models (Supplementary Material Table S1), we consider a crustal density of 2700 kg/m^3 (Whittington et al., 2009), a temperature-dependent thermal diffusivity as provided by Chapman and Furlong (1992) for the upper crust and a specific heat capacity calculated with Equations 3 and 4 of Whittington et al. (2009) (Supplementary Material Table S8). In order to evaluate the influence of the crustal thermal properties on the results obtained, we have also considered for specific models alternative temperature-dependent thermal diffusivity and specific heat capacity for the country rock (Supplementary Material Table S1). The latter are further described in Table S8 of the Supplementary Material.

The input temperature profile for the country rock is a typical geothermal gradient varying from 25 to 30ºC/km depending on the model (Supplementary Material Table S7) (Turcotte and Schubert, 2002). We assume a relatively uniform lateral temperature profile, and consider the surrounding walls of the country rock to have no heat flux (i.e. the outer edge of the rotationally symmetric model is insulating). The subcrustal mantle heat flow Q_{mantle} = 0.03 W/m^2 and the surface heat flow $Q_{surface}$ = 0.07 W/m^2 are assigned to the bottom and top limits of the computational domain, respectively (Fig. 1a) (Table 1). For the magma chamber, we assume an initial temperature T_{0_magma} equivalent to the liquidus temperature of the magma (Supplementary Material, Tables S2-S4).

Following the approach by Jellinek and DePaolo (2003) and Chen and Jin (2011), under high temperatures and confining pressures, crustal rocks are assumed to behave viscoplastically or also referred to as a solid-state creep flow. Thus, the host rock rheology can be described by the Weertman-Dorn power-law formulation where the relationship between strain rate and deviatoric stress is defined as follows (Jellinek and DePaolo, 2003 and references therein; Chen and Jin, 2011):

$$\dot{\varepsilon} = \left(\frac{d\varepsilon}{dt}\right)_v = Ke^{\frac{-G}{RT}}\sigma_v^n \quad \textbf{[2]}$$

where K is a constant that depends on the material, G is the activation energy for creep, n is the power law exponent, σ_v is the deviatoric stress, and R is the molar gas constant (Table 1). Interesting feature of this approach to the knowledge of the wall-rock rheology is that the effective wall-rock viscosity is an explicit function of temperature and strain rate (Jellinek and DePaolo, 2003). The thermal effects on the country rock are examined as a function of the temperature-dependent viscosity determined by the temperature field

distribution and calculated using the Arrhenius formulation (Del Negro et al., 2009; Chen and Jin, 2011; Gregg et al., 2012) :

$$v = A_D e^{(\frac{E_A}{RT})} \quad \textbf{[3]}$$

where A_D is the Dorn parameter (a material constant) and E_A is the activation energy (Table 1). According to Equation 2, higher temperatures close to the magma chamber-host rock boundary would implicate lower viscosities. Thus, the viscosity values of the heated aureole are expected to be much lower than the average viscosity estimates for continental crust (i.e. > 10^{19} Pa s).

2.2 Mineral assemblage prediction: phase diagram modeling

Magma chamber emplacement disrupts the temperature-dependent chemical equilibrium of the surrounding crust, triggering reactions to establish a new equilibrium. Thereby, we use thermodynamic modeling (P-T pseudosections) to predict equilibrium phase assemblages, reactions and modal changes occurring in the country rock around the magmatic body.

We use the thermodynamic database of Holland and Powell (1998, with updates) and Perple_X (Connolly, 2005) in the system Na_2O-CaO-K_2O-FeO-MgO-Al_2O_3-SiO_2-H_2O (NCKFMASH) (Fig. 2, Supplementary Material Figures S1 and S2). We consider three representative upper continental crustal compositions to simulate the magma emplacements effects on country rock, namely (Fig. 2, Supplementary Material Figures S1 and S2): (i) the anhydrous standard upper continental crust of Rudnick and Gao

(2003); (ii) a typical hydrous metapelite (Tinkham et al., 2001); and (iii) a metamarl (Miron et al., 2013). The growth of hydrated phases such biotite and cordierite in the standard continental crust requires a minimum amount of H_2O. Therefore, we include 0.25 of wt% water in the bulk composition of Rudnick and Gao (2003) to permit the formation of hydrated phases.

The activity–composition models for silicate melt (M), garnet (Grt) and biotite (Bt) are from White et al. (2007); staurolite (St), epidote (Ep) and cordierite (Crd) are taken from Holland and Powell (1998); plagioclase (Pl) and K-feldspar (Kfs) are from Holland (2003); calcite (Cc) is from Anovitz and Essene (1987); chlorite (Chl) is from Holland et al. (1998); and white mica (Ms, Pa, Ma) is from Coggon and Holland (2002).

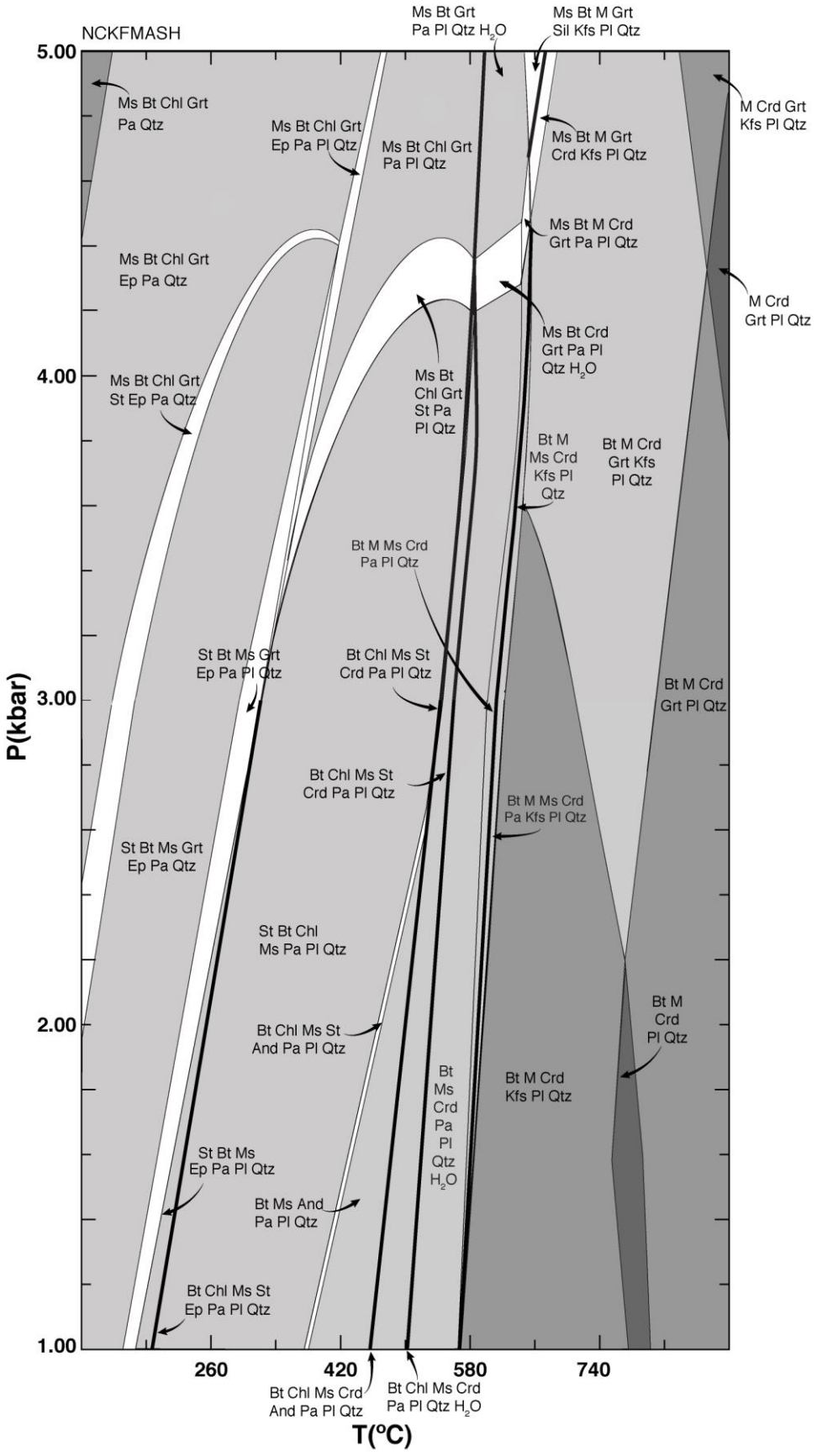

Figure 2 (1.5 column): *Pressure-Temperature pseudosection in the NCKFMASH system. Darker shading indicates higher variance. Bulk composition (wt.% normalized to 100) is of a hydrated metapelite from Tinkham et al. (2001): Na_2O: 1.65, CaO: 1.21, K_2O: 3.70, FeO: 6.87, MgO: 3.44, Al_2O_3: 16.88, SiO_2: 60.78, H_2O: 5.44. And (andalusite), St (staurolite); Bt (biotite); Ms (muscovite); Ep (epidote); Pa (paragonite); Pl (plagioclase); Qtz (quartz); M (melt); Crd (cordierite); Grt (garnet); Chl (chlorite); Kfs (K-feldspar).*

3. Results

We run a total of 14 simulations varying the crustal geothermal gradient, the initial magma composition, the magma reservoir geometry, volume and emplacement depth, and the host rock thermal properties (Supplementary Material Table S1). We arbitrarily select a reference model (hereafter referred to as *M_reference*) to evaluate how the above listed parameters influenced the results obtained. The latter consists of a rhyolitic, oblate magma chamber with a 100 km^3 volume centered on a depth equivalent to 3 kbar in a crust with 30ºC/km thermal gradient (Supplementary Material Table S1).

For each numerical simulation, we check the temperature field distribution and evolution along two profiles, D-D' and E-E' (Fig. 1a). In order to monitor their local metamorphic peaks, we select three representative points located at the top, bottom and edge of the magma chamber along the D-D' profile (Fig. 1a, points A to C). Finally, we superimpose the P-T pseudosections on the temperature and pressure fields of the host rock in order to visualize mineral equilibria evolution throughout the crust (see Figs. 3 to 6 for the most relevant results).

Peak temperatures along the D-D' profile are reached at the magma chamber bottom, independently of the model (Fig. 3a, label I). These may be up to ~878 ºC when

assuming a basaltic magma composition inside the reservoir (*M_comp_basalt* model, Supplementary Material Table S1). However, the highest temperature increase ΔT defined as:

$$\Delta T = T - T0\_crust \quad \textbf{[4]}$$

where *T0_crust* is the initial temperature of the country rock based on the imposed geothermal gradient, is always achieved at the top of the magma chamber (Fig. 3b, label II).

Results obtained along the E-E' profile (Fig. 4b) indicate that the temperature increase in the country rock due to the magmatic accumulation does not propagate to large distances from the host rock–reservoir contact. All models considering a magma chamber of 100 km^3 show that highest ΔT values (>200 ºC) are restricted to less than 150 meters from the contact (Fig. 3c, label III). If the modeled magma accumulation is of 1000 km^3 (*Model_volume_1000* model, Supplementary Material Table S1), the mentioned distance increases up to 510 m. This indicates that the spatial extent of the thermal effects directly relates to the magma chamber volume.

The reservoir geometry strongly influences the thermal behavior. For a spherical reservoir (*M_shape_sphere* model, Supplementary Material Table S1) the temperature around the magma chamber contour increases linearly with depth (Fig. 3a, label IV). Additionally, the thermal evolution is similar at all three control points with points A and B reaching their peak temperature nearly simultaneously at 0.47± 0.03 ka and point C at 0.60± 0.03 ka (Fig. 3d, label V). For oblate magmatic reservoirs, there is a systematic minimum temperature at the magma chamber's edge, i.e. the control point B (Fig. 3a, label VI). In the case of the reference model, maximum host rock temperatures at the magma chamber edge are reached much earlier (i.e. point B at 0.13 ± 0.03 ka; Fig. 3d,

label VII) than at the reservoir top (i.e. point A at 2.54 ±0.3 ka; Fig. 3d, label VIII) or bottom (i.e. point C at 13.00 ± 0.3 ka; Fig. 3d, label IX). Concerning the prolate chamber geometry (*M_shape_prolate* model, Supplementary Material Table S1), the metamorphic peak is reached first, and almost simultaneously, at the control points A and C (0.19± 0.03 ka, Fig. 3e, label X), and later at B (0.60± 0.03 ka, Fig. 3e, label XI). Further results regarding the influence of the studied parameters (i.e. host rock thermal gradient, reservoir volume and depth, thermal properties of the crust) on the temperature evolution through time at all three control points can be found at the Supplementary Material (Figs. S3 and S4).

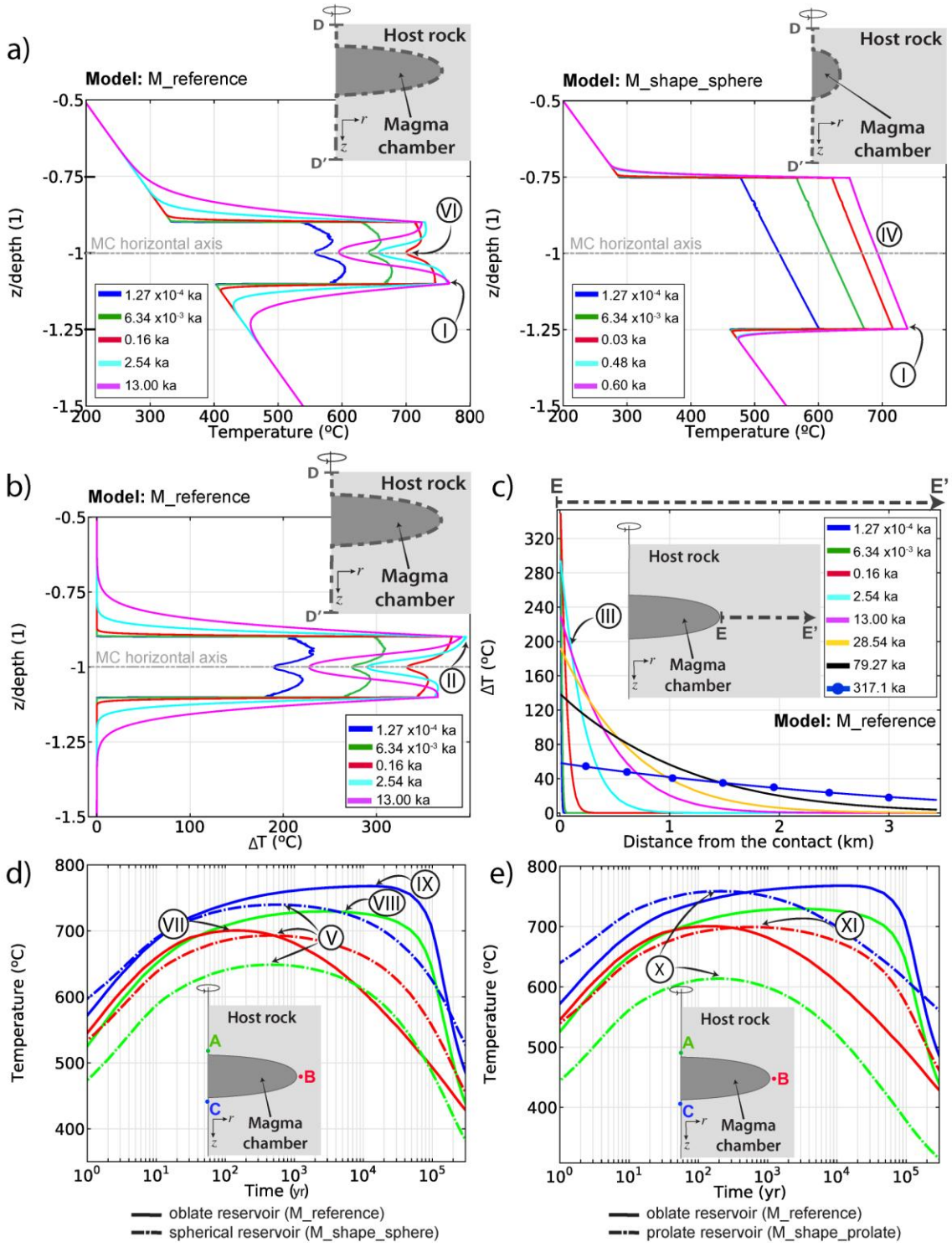

Figure 3 (double column): *Summary of the most relevant results discussed in the text regarding temperature distribution at the country rock due to the heated magma chamber. (a) Temperature distribution along the D-D' profile at different time steps.*

Results for the oblate (left) (M_reference model) *and spherical (right) (M_shape_spherical model) reservoir are illustrated. Depth z is normalized towards the magma chamber center depth d, i.e. z/depth = -1 indicates magma chamber horizontal axis. Temperature increase ΔT along the D-D' (b) and E-E' (c) profiles for the oblate reservoir (M_reference model). Comparison of the temperature evolution at the three control points (A-C) for the case of the oblate and spherical (d) and oblate and prolate (e) reservoirs (M_reference, M_shape_sphere and M_shape_prolate models, respectively). Model name as listed in Table S1 of the Supplementary Material indicated within brackets. Roman numerals detailed in the text.*

With regards to the viscosity changes of the country rock according to Equation 3, these are not uniformly distributed around the reservoir. For example, in the case of the reference model (i.e. oblate chamber), when control point C reached the highest temperature value (i.e. 768 ºC), ν is significantly lower at the magma chamber's top (1.92×10^{15} Pa s) and bottom (10^{15} Pa s) than at its edges (1.64×10^{16} Pa s) (Fig. 4a, label I). Results obtained along the E-E' profile show dramatic viscosity drops of one order of magnitude below the average crustal values (10^{19}-10^{21} Pa s). The lowest viscosity values calculated here ($\nu < 10^{16}$ Pa s) are restricted to the first 35m from the contact (Fig. 4b, label I). This distance increases up to 100m when assuming a prolate geometry (*M_shape_prolate* model, Supplementary Material Table S1) and to 2km for a reservoir volume of 1000km^3 (*Model_volume_1000* model, Supplementary Material Table S1).

The reservoir geometry strongly affects the viscosity values at the different control points in time. In the case of the reference model (i.e. oblate accumulation), the time during which the host rock at the three control points experiences viscosities below 10^{16} Pa s is orders of magnitude different: the control points located over and below the

reservoir exhibit low viscosity values ($\nu < 10^6$ Pa s) for over 100 ka, while the one located along the magma chamber's horizontal axis experiences such low viscosity values for only c. 7 ka (Fig. 4c). For the spherical reservoir, the length of time that the country rock at the control points exhibits viscosity values below 10^{16} Pa s increases gradually with depth (Fig. 4d). This trend is also observable for the prolate reservoir (Fig. 4e). However, in this case, the viscosity at control point A never drops below 10^{16} Pa s.

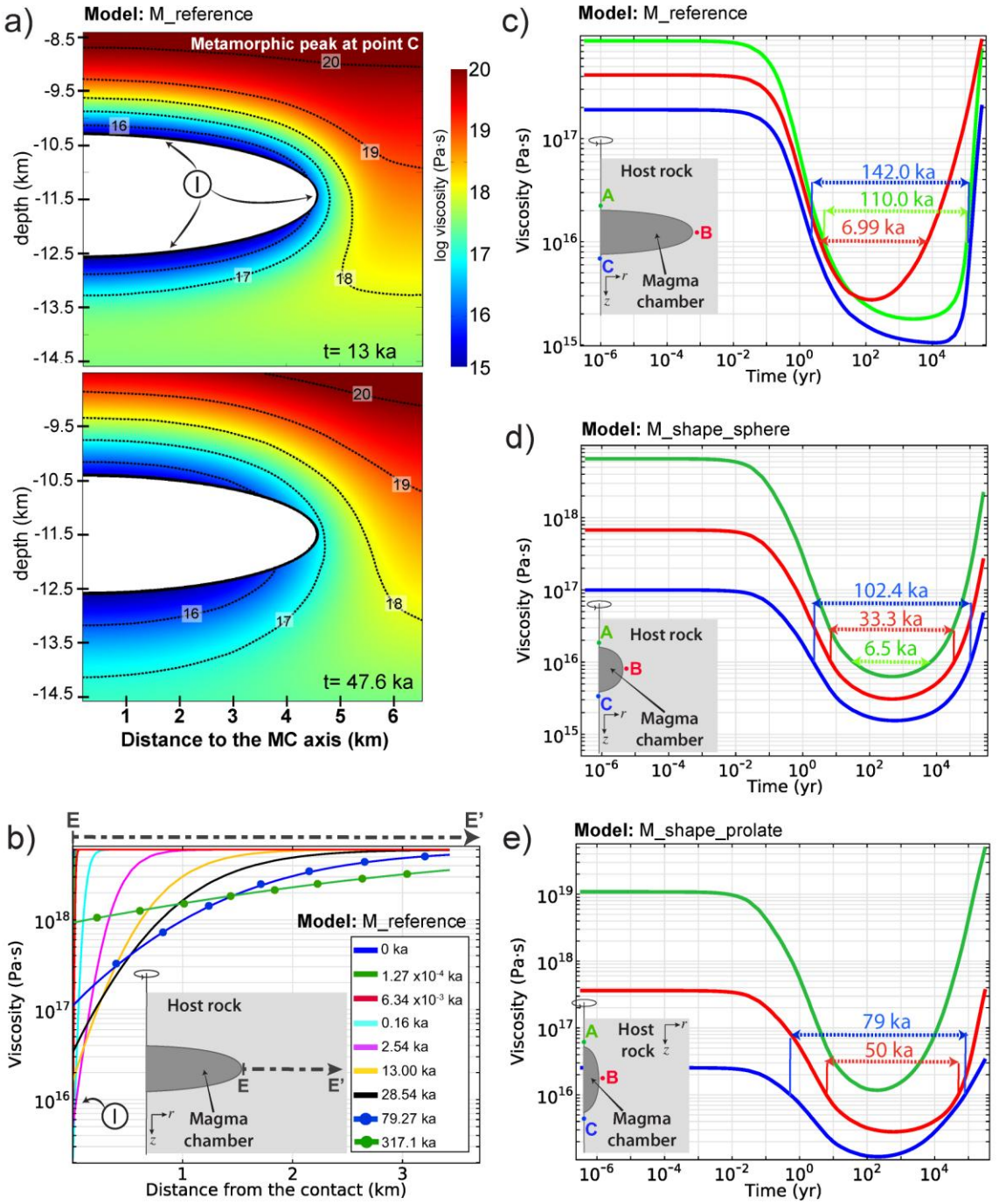

Figure 4 (double column): *Summary of the most relevant results discussed in the text regarding viscosity changes at the country rock due to the magma chamber accumulation. (a) Viscosity of the country rock at the metamorphic peak of point C for the reference model (M_reference, i.e. rhyolitic magma at 3 kbar depth). (B) Country rock viscosity along the E-E' crustal profile at different time steps for the reference*

oblate reservoir. Evolution of the country rock's viscosity at the three control points (A, B, C) for the oblate (c), spherical (d) and prolate (e) reservoirs (M_reference, M_shape_sphere and M_shape_prolate models, respectively). The dashed lines with double arrows indicate the time interval in which the control crustal points remain below viscosity value of 10^{16} Pa s.

Next, we examine how changes in the temperature field of the country rock influence the mineral equilibria of three different crustal compositions. For this purpose, we overlay the P-T pseudosections (Fig. 2; and Supplementary Material, Figures S1 and S2) on the temperature and pressures given by the numerical simulations (Fig. 5).

The thickness and grade of mineral equilibria in the metamorphic aureole vary with time and strongly depend on the reservoir's geometry, typically displaying significant differences between the bottom and top of the magma chambers (e.g. Fig. 5a, label I). The prolate reservoir, which has the greatest pressure difference between top and bottom of the chamber (c. 2.5 kbar), presents the highest range of metamorphic mineral reactions (Fig. 5c). Control point B (i.e. in the horizontal axis of the magma chamber and located at nearly the same pressure) shows similar petrologic changes within the contact aureole independent of reservoir geometry (Fig. 5, label II). The thickness of the contact aureole is also influenced by the reservoir shape, extending ca. 240 m and 90 m for the oblate (Fig.5a, label III) and spherical (Fig. 5b, label IV) reservoirs, respectively.

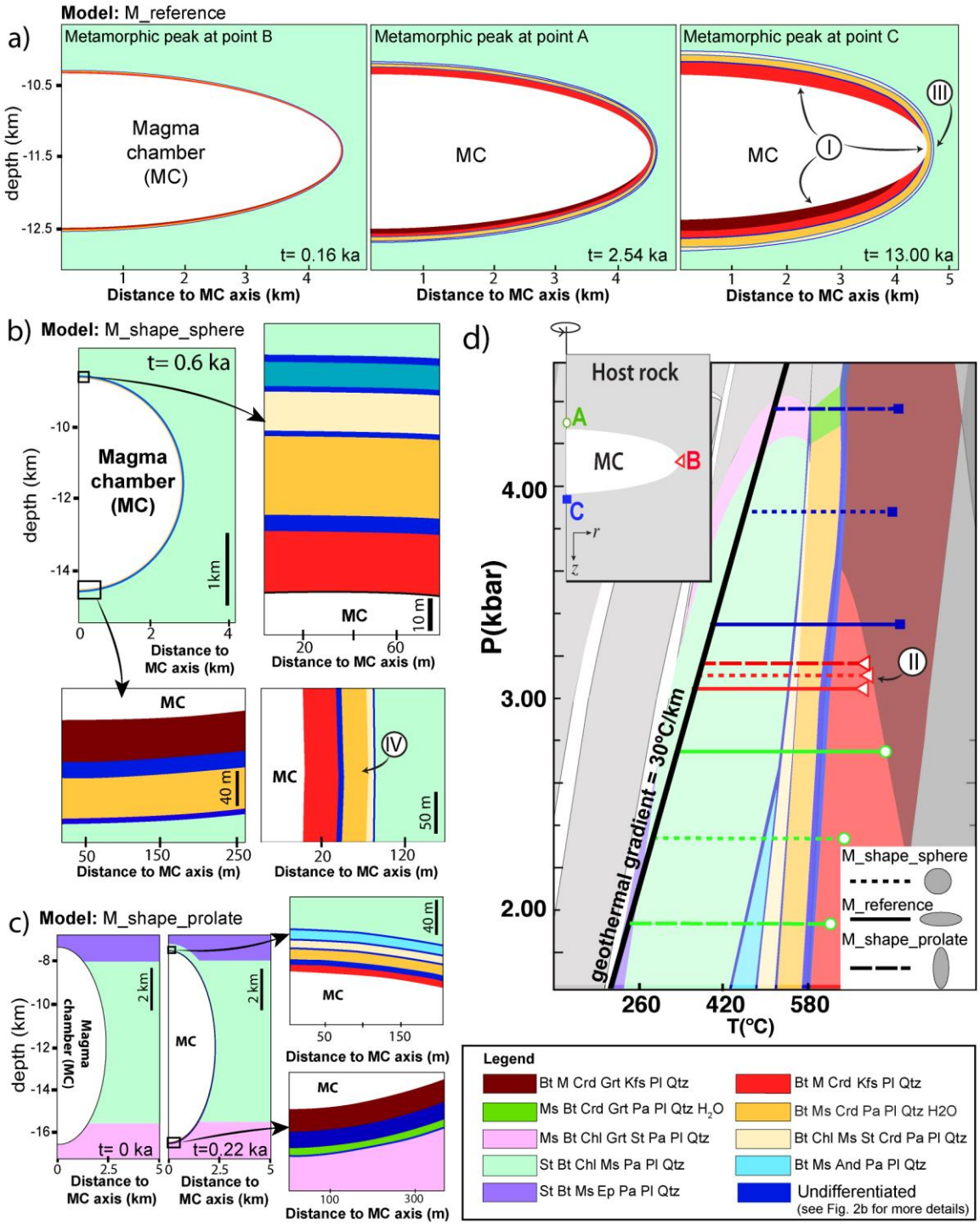

Figure 5 (double column): *(a) Evolution of the metamorphic aureole for the reference model at different time steps corresponding to the metamorphic peak of the three control points: A, B and C. (b) Predicted mineral assemblage for the case of a spherical reservoir. The time step corresponds to the metamorphic peak of point C (i.e. magma*

chamber bottom). (c) The same for the prolate reservoir at t= 0s and at the metamorphic peak of C (i.e. magma chamber bottom). (d) For illustrative purposes we also show the predicted mineral assemblage for the metapelitic crust color-coded for the different phases identified in the results shown in (a), (b) and (c). The green, red and blue horizontal lines indicate the temperature increase experienced at the top (control point A), horizontal axis (control point B) and bottom (control point C) of the magma chamber in the case of the spherical (dotted lines), oblate (solid lines) and prolate (dashed lines) reservoirs. Roman numerals are detailed in the main text. And (andalusite), St (staurolite); Bt (biotite); Ms (muscovite); Ep (epidote); Pa (paragonite); Pl (plagioclase); Qtz (quartz); M (melt); Crd (cordierite); Grt (garnet); Chl (chlorite); Kfs (K-feldspar).

We also run the same simulations for two other crustal compositions including: (i) a crustal metamarl (Supplementary Material, Fig. S2), which shows a similar metamorphic trend to the described above for the metapelitic case but with different mineral assemblages; (ii) a typical upper crust (Rudnick and Gao, 2003), which shows no contact metamorphic changes as the P-T evolution of the three control points are stable within the same equilibrium mineral assemblage (Supplementary Material Fig. S1).

4. Discussion

4.1 Numerical modeling of heat transfer from the magma chamber to the surrounding crust

There is a general agreement when computing numerical simulations of cooling evolution in a magma chamber, about the restrictions or simplifications that may potentially influence the estimates of the thermal effects in the surrounding host rock. On

this regard, many of the existing numerical models so far: (i) simulate the reservoir as a pressurized cavity with a constant heat flux to the country rock (e.g. Jellinek and De Paolo, 2003); (ii) assume the thermal properties to keep constant values, including diffusivity and specific heat capacity for a constant P, regardless of T (e.g. Gottsmann and Odbert, 2014); (iii) ignore the existence of hydrothermal fluids in the country rock (e.g. Gregg et al., 2012); (iv) consider just the conductive term of the heat transfer equation assuming that no convection is taking place inside the magma chamber (e.g. Gelman et al., 2013); (v) consider the magma reservoir to be instantaneously emplaced (e.g. Gutiérrez and Parada, 2010); and (vi) ignore endothermic metamorphic reactions occurring in the country rocks during the thermal evolution of the aureole (e.g. Jellinek and De Paolo, 2003).

Concerning the first simplification, i.e. considering constant heat flux from the magma chamber uniformly distributed along the reservoir-host rock contact, it leads to an overestimation of the thermal effects at the country rock (e.g. Gregg et al. 2012). Yet the heat flux from the magma chamber to the country rock is high at the beginning of the magma-cooling episode, but rapidly decreases as the reservoir cools down (Fig. 6). Hence, keeping the thermal heat flux constant during the simulation leads to an overheating of the country rock over long periods of time, which translates in to an overestimate of the thermal aureole's size and duration.

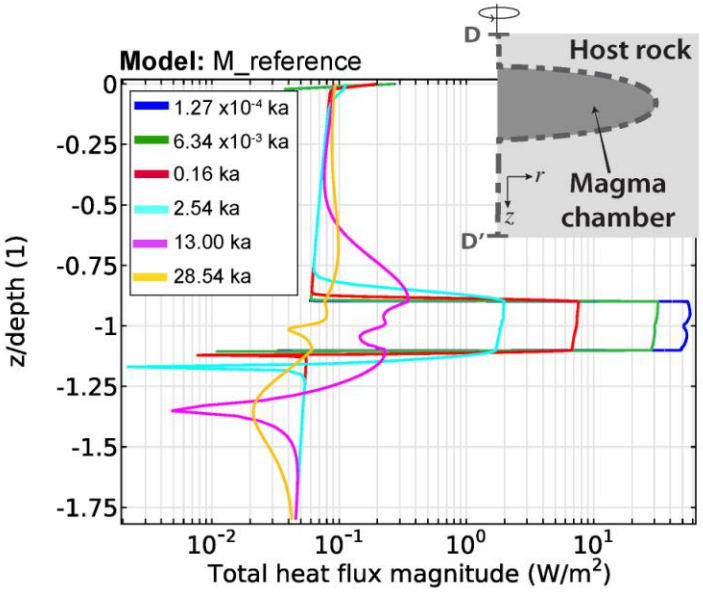

Figure 6 (single column): *Heat flux along the D-D' profile at 5 m from the magma chamber – host rock contact for different time steps. Depth z is normalized towards the magma chamber center depth d, i.e. z/depth = -1 indicates magma chamber horizontal axis. Results correspond to those obtained with the reference model (M_reference).*

The second assumption of temperature-independent thermal properties of the magma and country rock limits the model's accuracy in describing thermal evolution over large temperature ranges. The numerical simulations presented by Nabelek et al. (2012) demonstrated that the modeled longevities of magmatic systems are significantly extended by accounting for thermal dependencies in material properties. The time for the magma solidification is long because of both its low thermal diffusivity and the wall rocks become more insulating as temperature rises (Whittington et al., 2009, Supplementary Material Table S8). Thus, the temperature increase rate and the duration of elevated temperature regimes in the country rock are affected. According to Nabelek et al. (2012), assuming constant diffusivity values does not significantly impact peak temperature values at any location in the country rock. However, once the country rocks

are heated up and their thermal diffusivity decreases, they remain at high temperatures for longer than in models assuming a constant thermal diffusivity (Nabelek et al., 2012).

As mentioned in the methodology section, our models overcome the first two restrictions. The temperature-dependent thermal properties of the crust are considered to be homogeneous among the whole computational domain (i.e. crustal section). However, results obtained when changing the thermal properties of the crust (Supplementary Material Table S8) indicate that variations in the thermal diffusivity and specific heat capacity may influence the thermal evolution of the country rock, especially the temperature value at the metamorphic peak (Supplementary Material Figure S4). Therefore, when working with real case studies, the implementation of a proper numerical model considering the individual geologic units and their specific temperature-dependent thermal properties is strongly recommended (e.g. Cook and Bowman, 1994; Cui et al. 2001, Álvarez-Valero et al., 2015; Pla and Álvarez-Valero, 2015). This would allow accounting for variations of the thermal properties due to changes of the host rock composition, water content, porosity, etc.

Regarding the third and fourth limitations, i.e. not including magma convection within the chamber as well as neglecting the presence of fluids in the country rock, their effects on the outcomes are still under discussion. On the one hand, internal magmatic convection has been shown to affect peak temperatures in the contact aureole (Jaeger, 1964;Cook and Bowman, 1994). These effects are expected to be minor on distance profiles normal to the igneous contacts of planar or regular geometries, except when being either close to the reservoir-rock contact (Bowers et al., 1990), or next to local reservoir irregularities, such as re-entrants and apophyses (Cook and Bowman, 1994).

Bowers et al. (1990) demonstrated that magmatic convection can also result in isotherm geometries that significantly differ from pure conduction, causing isotherms near the igneous contact to conform more closely to the shape of the reservoir. On the contrary, Bergantz and Dawes (1994) argued that given a realistic set of parameters and boundary conditions, those models considering convection inside the magma chamber do not give fundamentally distinctive results from purely conductive ones. Thus, this evidences that the influence of the convective processes inside the magma chamber is not well understood yet and should be analyzed in future works by taking into account as starting point, for example, the works by Bea (2010), Gutierrez and Parada (2010) or Koyaguchi and Taneko (2000).

Regarding the effects of fluids in the country rock during thermal cooling processes, conductive heat transfer seems to play the prevailing role in the evolution of the aureole (Johnson et al., 2011). However, the country rock permeability and amount of fluids seem to control the degree to which conduction or convection may dominate the system (Johnson et al., 2011). The aureoles of intrusions emplaced at shallow crustal levels are most likely to experience significant heat transfer through fluid convection, owing to the higher permeability of wall rocks and the greater availability of significant fluid volumes, including meteoric waters (see Johnson et al., 2011 and references therein). At depths greater than ~8–10 km, as in our models, the role of fluid convection diminishes significantly due to decreased permeability and fluid availability (cf. Johnson et al., 2011)

Probably the most remarkable oversimplification in our models is that the cooling magma is emplaced instantaneously in the crust, i.e. we are not modeling the

emplacement and growth of the chamber, but once is already accumulated within the upper crust. Hence, we are not considering possible thermal effects occurring during magma ascent and emplacement. Numerous authors also assumed this simplification presumably because of numerical limitations but also due to the fact that the main mechanisms of magma transport and emplacement into the crust are not fully understood (e.g. Gregg et al., 2012;Gottsmann and Odbert, 2014). From diapirism to hydrofracturing (dyke injection), there are several theories aimed to explain how magma arrives at shallow crustal levels and starts accumulating (e.g. Petford and Clemens, 2000; Petford et al., 2000). Considering the recent results by Keller et al. (2013), the change from one mechanism to the other, would mainly depend on the host rock viscosity and tensile strength. Numerical models combining transport, emplacement and magma cooling have been recently developed by Gelman et al. (2013). They simulated formations of large magmatic reservoirs by periodic accumulations (controlled by the injection rate) of new magma pulses at the bottom of the reservoir. Their results allowed to quantitatively assessing the heat balance between a crystallizing magma and the surrounding crust as it is periodically rejuvenated by hot recharge from below (cf. Gelman et al., 2013). They did not focus on how the accumulating sills may thermally affect the country rock, but on inferring the necessary injection rates to keep melting the upper crust and form huge (>500 km^3) batches of mobile silicic magma. We assume that this aspect will depend on the sill size, the injection rate and the thermal properties of the crust. Future works are needed to investigate the thermal effects on the country rock due to magma intrusions based on the way the latter accumulates in the crust either as large single batch or as periodic sill injections.

Finally, our preliminary models allow to broadly constraining the potential feedback between petrological and mechanical changes. Despite this requires a further and detailed study of the endothermic reactions record in the host rock to be incorporated into the numerical simulations, our calculated temperature regimes and predicted petrological changes represent a novel advance on this purpose. As indicated in previous works, the incorporation of metamorphic endothermic reactions into the numerical simulations decreases the overall temperature throughout the aureole (Cook and Bowman, 1994) by consuming a significant quantity of heat (Ferry, 1980). This effect was investigated in the Cupsuptic pluton (Main, United States) by Bowers et al. (1990) (Fig. 7). They included the chlorite dehydratation reaction in their numerical simulations, which represents the greatest heat sink of all endothermic reactions taking place around the Cupsuptic pluton. Their results also indicated that incorporating this metamorphic reaction leads to a thinner contact aureole (Figure 7a, label I) and to slightly different geometrical distribution of the maximum temperatures around apophyses and pluton's geometrical irregularities (Fig. 7a, labels II and III). However, they also showed that the general shapes of the maximum temperature isotherms were poorly affected. Regarding the maximum temperatures achieved at any point around the pluton, the no inclusion in the numerical simulations of the endothermic reactions may lead to an overestimation of temperature by as much as 40-50 ºC (Fig. 7b). Bowers and co-workers considered a non-constant latent heat of crystallization that decreases with temperature (Fig. 7c). Therefore, with time, the endothermic dehydration reaction of chlorite becomes more important than latent heat in affecting the temperature distribution around the aureole (Fig. 7c).

In summary, our calculated temperature regimes and predicted petrological

changes (e.g. Fig. 5) have to be considered as maximum estimates. Due to the nature of the Arrhenius formulation (Eq. 3), to what extent a 40-50 ºC temperature difference influences the calculated viscosity for the country rock depends significantly on temperature. Thus, for low temperatures, e.g. passing from 400 to 350 ºC, a 50 ºC disparity would translate in a viscosity increase of nearly one order of magnitude, ranging from 2.05×10^{18} to 1.15×10^{19} Pa s. However, at higher temperatures, a temperature drop of 50ºC (i.e. from 900 to 850 ºC) has minor consequences for the viscosity, which just increases from 2.20×10^{13} to 3.81×10^{13} Pa s. Accordingly, differences in the numerical results due to the endothermic reactions will have a lesser effect close to the contact magma chamber-host rock and at the metamorphic peak, where temperatures are much higher.

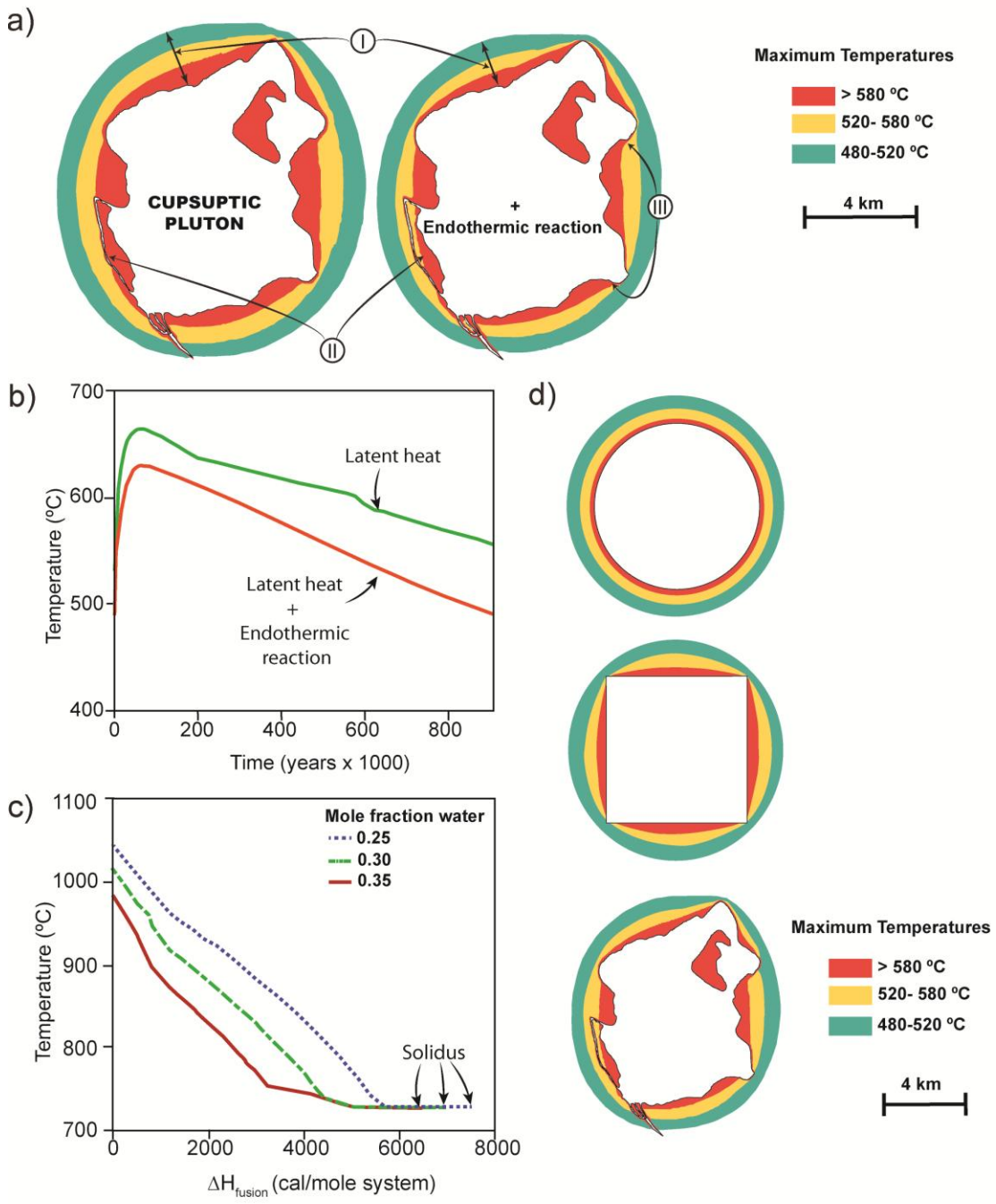

Figure 7 (double column): *(a) Results for the thermal conduction model of the Cupsuptic pluton carried out by Bowers and co-workers (1990). The left figure shows maximum temperature isotherms computed including effect of the 35 cal/ g of latent heat released non-linearly according to the crystallization model of Nekvasil as shown in (c). The right figure includes both latent heat and the effect of the 20 cal/g endothermic*

chlorite dehydration reaction in the aureole. (b) Time-temperature curves at a distance of 40 m from the contact illustrating the consequences on temperature distribution of including latent heat of fusion and the biotite isograd endothermic reaction in the numerical simulations (c). Curves for latent heat released with temperature decrease for Cupsuptic melt with 0.25, 0.30, and 0.35 mole fraction water (computed by H. Nekvasil, in Bowers et al., 1990). (d) Maximum temperature isotherms obtained from two-dimensional conduction heat flow models of an infinite cylinder (left), an infinite parallelepiped (center) and Cupsuptic intrusion (right) (all figures modified from Bowers et al., 1990).

4.2 Rheological effects

It is well known that temperature can affect the rock's rheology in different ways. The general tendency of temperature is to decrease the modulus of elasticity and make the rock become more viscous and ductile, and even more plastic. More specifically, an increase in temperature tends to low the von Mises yield stress for ductile behavior reducing the pressure of brittle - ductile transition and the field of brittle behavior for materials (Jaeger et al., 2007).

In the last years, numerous studies in volcanology have focused on how the thermal effects of magma accumulations alter the local country rock thermomechanics (e.g. Jellinek and De Paolo, 2003; Gregg et al., 2012, 2013). According to previous works, viscosity drops related to temperature increase may convert part of the brittle host rock around the intrusion into a ductile shell (e.g. Jellinek and De Paolo, 2003;Currenti and Williams, 2014;Gottsmann and Odbert, 2014). As a direct consequence of this, Jellinek and DePaolo (2003) pointed out that viscous deformation of wall rocks may

influence the dynamics governing the formation of dikes. Their numerical simulations indicate that this phenomenon is strongly controlled by the influx of new magma into the chamber, the reservoir volume, and the country rock rheology. On the one hand, chambers of less than 100 km^3, with relatively cool wall rocks, can be pressurized up to the critical overpressure needed to form and propagate dikes from the chamber to the surface (i.e. ~10-40 MPa) (Fig. 8a). On the contrary, assuming a typical magma supply rate, larger reservoirs capable of heating the country rock to a great extent, cannot achieve this overpressure. Subsequently, there is a strong tendency for magma to accumulate in the chamber, which will continue growing in volume as new magma arrives. Jellinek and DePaolo (2003) stated that it may not be necessary that the viscous regime develops around the entire magmatic reservoir, but just with a substantial fraction of the chamber walls the reservoir would not be able to reach the critical overpressure necessary for a magma chamber's rupture and subsequent dike's injection. Nonetheless, their results may vary depending on the magma chamber geometry, e.g. large chambers may also produce dikes if they are horizontally elongated, since extensional stresses generated by overpressure concentrate at those sections of the chamber wall with higher curvature (Jellinek and DePaolo, 2003).

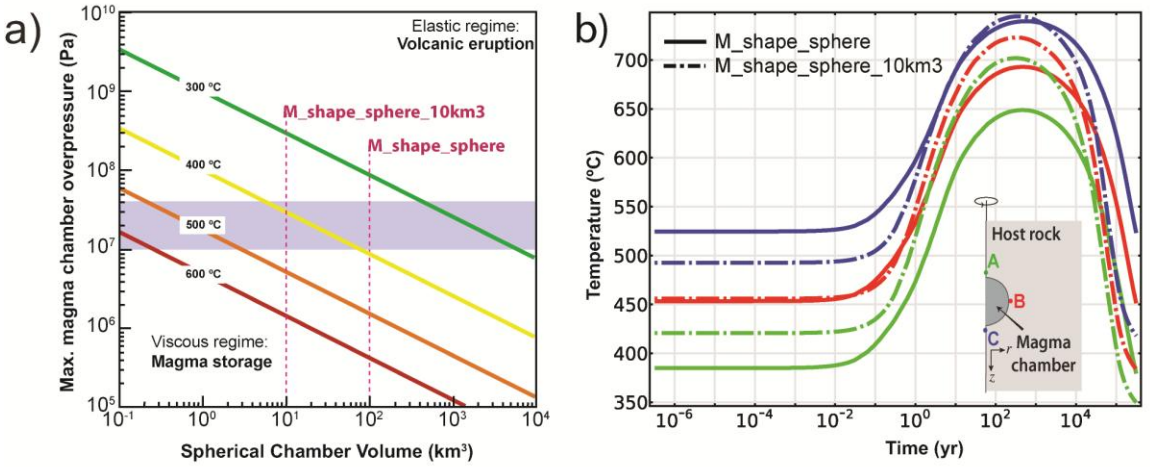

Figure 8 (double column): (a) The maximum chamber overpressure generated by a constant magma influx of Q=0.005 km^3 / year, as a function of chamber volume for a spherical chamber contained in rocks with a power law rheology according to Eqs. 2 and 3. The shaded region shows the probable range of critical overpressures required to propagate a rhyolite dike to the surface and delineates regimes leading to magma storage or volcanic eruption (modified from Jellinek and DePaolo, 2003). (b) Comparison of the temperature evolution at the three control points (A-C) for the case of spherical reservoir of 100km^3 (M_shape_sphere) and the one of 10km^3 (M_shape_sphere_10km3).

Since calculations by Jellinek and DePaolo (2003) are carried out assuming spherical magma chambers of various volumes, we can use their results to interpret our models considering spherical reservoirs (*M_shape_sphere* and *M_shape_sphere_10km3* models) (Fig. 8a). We can observe that according to their simulations, the 100km^3 and 10 km^3 magma chambers could reach the critical overpressure for a dike's injection at temperatures below ~400ºC or 450ºC in the country rock, respectively. For both of our models, nearly after the cooling process starts (< 1 year) close to the magma chamber-host rock contact, the rock is already heated over 450ºC reaching up to 750 ºC at the metamorphic peak (Fig. 8b). This implies that the developed ductile thermal aureole is

expected to inhibit the dyke's injection and the magma chamber's rupture, as well as promoting the growth of the reservoir (Dragoni and Magnanensi, 1989;Jellinek and De Paolo, 2003).

This later assumption is apparently in contradiction to what we observe during typical volcanic crisis or unrest events, where the recorded seismicity corresponds to brittle failure (hydrofracturing) of the magma reservoir (e.g. Martí et al., 2013). Thus, how can we explain the apparent discrepancies between the natural observations and the numerical results? A simple answer may be the different assumptions applied in the numerical simulations. However, none of the assumptions described above leads to a complete disappearance of a thermal aureole, not give answers to which is thinner or wider, which developed sooner or later and (according to Equation 3) leading to a relevant viscosity drop. So, either all existing models, or the interpretations drawn from the obtained results are not fully constrained. We consider that this aspect has to be properly addressed in the future, putting especial interest on the fact that a quite simple formulation as the one expressed in Equation 3, may not be enough to accurately describe the natural processes taking place. For example, other aspects such as changes in the yield strength with increasing temperature should be also evaluated in future works.

We think that even if there is a viscosity drop of the host rock around the reservoir, is not clear that this ductile shell may inhibit dyke injection or caldera-formation as indicated by previous authors (e.g. Dragoni and Magnanensi, 1989;Gregg et al., 2012). Even if this viscosity drop in the country rock is interpreted as a transition to ductile behavior, this does not mean that brittle fracturing from the magma reservoir is not possible to occur. We consider that this is only valid for low deformation rate

processes, such as for example, slow magma chamber replenishment. However, due to high deformation rates the country rock is likely able to fracture in a brittle manner.

4.3 *Mineralogical changes*

Our numerical combining approach of petrological and thermal modeling is new in the volcanology's literature.. While it is widely accepted that large igneous accumulations are frequently associated with contact aureoles, the relation between petrological and mechanical regime changes has not been thoroughly investigated. Intuitively, these changes are correlated due to their similar dependence on temperature, but due to local conditions may not be directly linked.

Our results reveal that for a given magma reservoir geometry and type of host rock, the thermal effects may or not be correlated to petrological changes. For instance, the spatial distribution of the ductile halo and contact aureole do not correspond in the case of a compositionally average upper crust, such as the one of Rudnick and Gao (2003). Since the whole magma body and immediate surrounding host rock fall within the same Bt-Grt-Ab-Kfs-An-Qtz stability field, an increase of the host rock temperature due to the magma accumulation predicts no mineralogical changes based on phase diagram modeling (Supplementary Material Figure S1). Thus, while Equation 3 foresees the existence of a viscous shell around the magma reservoir (Fig. 9a), this may not leave a visible contact aureole due to petrologic alteration. This relation is a direct result of the upper crust standard composition used for the P-T pseudosections. While the crustal composition from Rudnick and Gao (2003) is commonly used in numerical simulations,

these results indicate that using an average crustal composition may not provide accurate petrologic predictions for a local, rapidly changing thermal gradient.

The fact that thermal effects on the host rock viscosity are not necessarily related to petrological changes (e.g. Fig. 9a, label I), is crucial when attempting to reconstruct the magmatic history of a specific magma chamber based on field evidence. Hence, even if contact metamorphism is restricted to a short distance from the magma chamber contact, rheological changes triggered by the temperature increase may extend significantly further into the country rock (Fig. 9a). This is especially important for spherical and prolate reservoirs, where the metamorphic front is poorly developed but viscosity varies over a few orders of magnitude along the magma body's contour (Fig. 9b and c, label II). In addition, after the metamorphic peak, the thermal effects continue propagating further from the magma chamber contact while the petrological changes begin to regress (Fig. 4a).

Of high importance is the effect of the reservoir geometry on the shape and extent of the metamorphic aureole. This phenomenon, already observed by other authors (e.g. Bowers et al., 1990) (Fig. 7d), requires special attention when reconstructing the thermal evolution of plutons based on field studies. It may happen that field observations of the contact aureole may be scarce or not representative enough. Thus, when working on real case studies, it is necessary to have, as detailed as possible, a full description of the original geometry and size of the pluton to be able to get a complete picture of the cooling history of the igneous intrusion.

We conclude that through the combination of the numerical and petrological models, the magma chamber shape and crustal composition are, key parameters,

controlling the distribution and evolution of both the contact metamorphism aureole and the thermal effects.

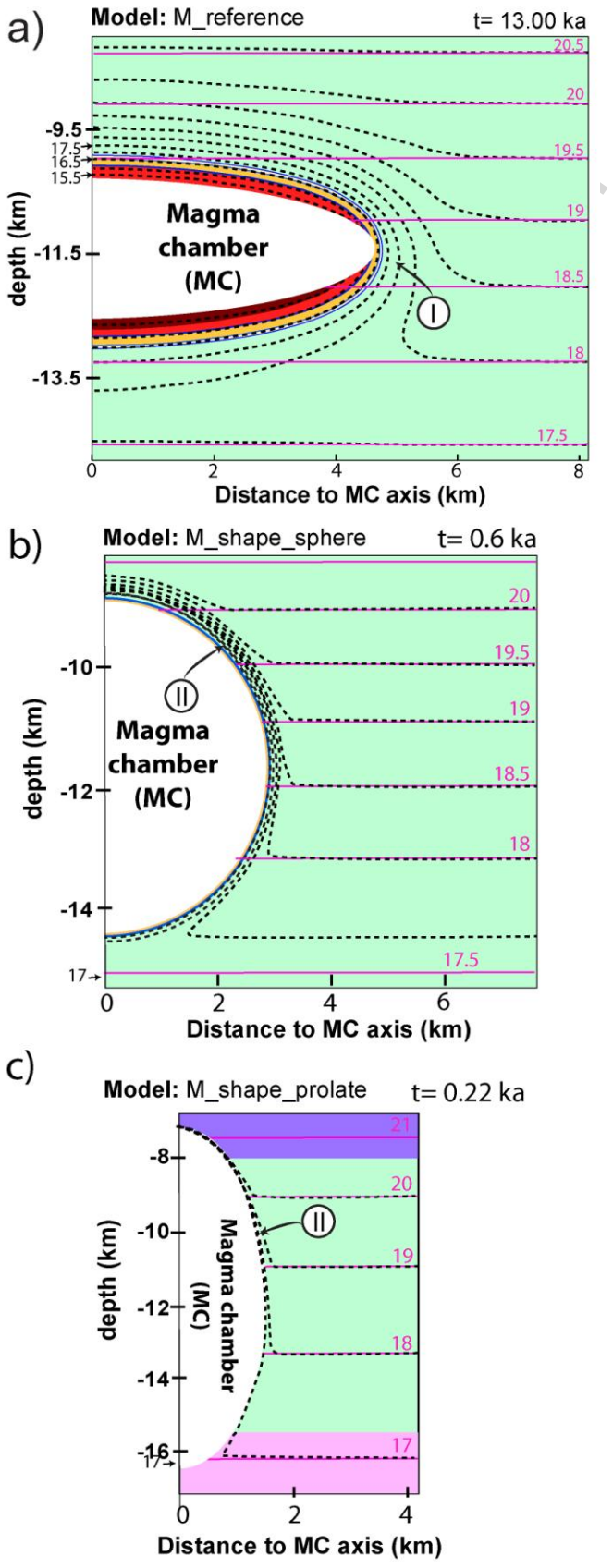

Figure 7 (single column): *Combination of the petrological and thermomechanical results for the different reservoir geometries. Colored areas correspond to the predicted mineral assemblage at the metamorphic peak of C for each model (color code as in Fig.5), and the magenta solid and the black dashed lines indicate the log10 of the host rock viscosity (in Pa s) t t=0s (i.e. T = T0_crust , initial crustal temperature based on the imposed geothermal gradient) and at the indicated time step , respectively. Roman numerals detailed in the text*

5. Summary and Conclusions

This study aims to understand how petrological and thermal changes relate to each other and affect the country rock after a magmatic accumulation. We numerically model both (i) the conductive cooling of an instantaneously emplaced magma chamber into compositionally representative pelitic and carbonatic upper crusts, and (ii) the changes in the viscosity of the host rock. Our predictions of the temperature field distribution at different time steps are integrated with modeled phase diagrams to investigate the metamorphic effects on the surrounding crust.

Our results indicate that the geometry of the magma accumulation plays a dominant role in controlling the local impacts of contact metamorphism and the thermal effects on the country rock, and we conclude that:

(i) The combination of relatively simple geothermal models with petrologic datasets can help to understand the maximum metamorphic grade and geometry of magma chamber aureoles;

(ii) The possible changes in the mechanical properties of the country rock are not necessarily linked to petrological changes within a contact aureole;

(iii) The present outcomes may be used in further studies of magma chamber stability and integrity, which may favor potential melt transfer throughout the crust.

6. Acknowledgments

AG is grateful for her Ramón y Cajal contract (RYC-2012-11024). A-V thanks the assistance of the "Ramón y Cajal" research program (MINECO 2011) and Programa Propio I (USal-2014). MD acknowledges the MISTI program (Massachusetts Institute of Technology [MIT] International Science and Technology Initiative) for funding work at the University of Salamanca in 2014. The authors are grateful to Carmen Rodríguez and an anonymous reviewer for their insightful comments and review of the manuscript, which have helped us improve this work. We also thank the Editor Lionel Wilson for his comments and for handling this paper.

References

Álvarez-Valero, A.M., Pla, F., Kriegsman, L.M., Geyer, A., and Herrero, H. (2015). Observing silicic magma transport in dykes at depths of 8-19km: Evidences from crustal xenoliths and numerical modelling. *Journal of Volcanology and Geothermal Research* 296**,** 69-79. doi: 10.1016/j.jvolgeores.2015.02.013.

Annen, C., Scaillet, B., and Sparks, R.S.J. (2006). Thermal Constraints on the Emplacement Rate of a Large Intrusive Complex: The Manaslu Leucogranite, Nepal Himalaya. *Journal of Petrology* 47**,** 71-95. doi: 10.1093/petrology/egi068.

Anovitz, L.M., and Essene, E.J. (1987). Phase Equilibria in the System CaCO3-MgCO3-FeCO3. *Journal of Petrology* 28**,** 389-415. doi: 10.1093/petrology/28.2.389.

Bea, F. (2010). Crystallization Dynamics of Granite Magma Chambers in the Absence of Regional Stress: Multiphysics Modeling with Natural Examples. *Journal of Petrology*, 51(7): 1541-1569. doi: 10.1093/petrology/egq028

Bergantz, G.W., and Dawes, R. (1994). "Aspects of magma generation and ascent in continental lithosphere," in *Magmatic systems*, ed. M.P. Ryan. (San Diego, CA: Academic Press), 291–317.

Bowers, J.R., Kerrick, D.M., and Furlong, K.P. (1990). Conduction model for the thermal evolution of the Cupsuptic aureole, Maine. *American Journal of Science* 290**,** 644-665. doi: 10.2475/ajs.290.6.644.

Bufe, N.A., Holness, M.B., and Humphreys, M.C.S. (2014). Contact Metamorphism of Precambrian Gneiss by the Skaergaard Intrusion. *Journal of Petrology* 55**,** 1595-1617. doi: 10.1093/petrology/egu035.

Carrigan, C.R. (1983). A heat pipe model for vertical, magma-filled conduits. *Journal of Volcanology and Geothermal Research* 16**,** 279-298. doi: 10.1016/0377-0273(83)90034-3.

Carrigan, C.R. (1988). Biot number and thermos bottle effect: Implications for magma-chamber convection. *Geology* 16**,** 771-774. doi: 10.1130/0091-7613(1988)016<0771:bnatbe>2.3.co;2.

Chapman, D.S. and Furlong, K.P., (1992). Continental Lower Crust. In: D.M. Fountain, R. Arculus and R.W. Kay (Editors), pp. 179-199.

Chen, Z. and Jin, Z.-H., 2011. Subcritical dyke propagation in a host rock with temperature-dependent viscoelastic properties. Geophysical Journal International, 186(3): 1095-1103. doi: 10.1111/j.1365-246X.2011.05113.x

Coggon, R., and Holland, T.J.B. (2002). Mixing properties of phengitic micas and revised garnet-phengite thermobarometers. *Journal of Metamorphic Geology* 20**,** 683-696. doi: 10.1046/j.1525-1314.2002.00395.x.

Connolly, J.a.D. (2005). Computation of phase equilibria by linear programming: A tool for geodynamic modeling and its application to subduction zone decarbonation. *Earth and Planetary Science Letters* 236**,** 524-541. doi: 10.1016/j.epsl.2005.04.033.

Cook, S.J., and Bowman, J.R. (1994). thermal constraints and evidence of advective heat transport from calcite + dolomite geothermometry. *American Mineralogist* 79**,** 513-525.

Costa, A., Sparks, R.S.J., Macedonio, G., and Melnik, O. (2009). Effects of wall-rock elasticity on magma flow in dykes during explosive eruptions. *Earth and Planetary Science Letters* 288**,** 455-462.

Cui, X., Nabelek, P.I., and Liu, M. (2001). Heat and fluid flow in contact metamorphic aureoles with layered and transient permeability, with application to the Notch Peak aureole, Utah. *Journal of Geophysical Research: Solid Earth* 106**,** 6477-6491. doi: 10.1029/2000jb900418.

Currenti, G., and Williams, C.A. (2014). Numerical modeling of deformation and stress fields around a magma chamber: Constraints on failure conditions and rheology. *Physics of the Earth and Planetary Interiors* 226**,** 14-27. doi: 10.1016/j.pepi.2013.11.003.

Del Negro, C., Currenti, G., and Scandura, D. (2009). Temperature-dependent viscoelastic modeling of ground deformation: Application to Etna volcano during the 1993-1997 inflation period. *Physics of the Earth and Planetary Interiors* 172**,** 299-309. doi: 10.1016/j.pepi.2008.10.019.

Dragoni, M., and Magnanensi, C. (1989). Displacement and stress produced by a pressurized, spherical magma chamber, surrounded by a viscoelastic shell. *Physics of the Earth and Planetary Interiors* 56**,** 316-328. doi: 10.1016/0031-9201(89)90166-0.

Ferry, J.M. (1980). A case study of the amount and distribution of heat and fluid during metamorphism. *Contributions to Mineralogy and Petrology* 71**,** 373-385. doi: 10.1007/bf00374708.

Fjeldskaar, W., Helset, H.M., Johansen, H., Grunnaleite, I., and Horstad, I. (2008). Thermal modelling of magmatic intrusions in the Gjallar Ridge, Norwegian Sea: implications for vitrinite reflectance and hydrocarbon maturation. *Basin Research* 20**,** 143-159. doi: 10.1111/j.1365-2117.2007.00347.x.

Galushkin, Y.I. (1997). Thermal effects of igneous intrusions on maturity of organic matter: A possible mechanism of intrusion. *Organic Geochemistry* 26**,** 645-658. doi: 10.1016/S0146-6380(97)00030-2.

Gelman, S.E., Gutiérrez, F.J., and Bachmann, O. (2013). On the longevity of large upper crustal silicic magma reservoirs. *Geology* 41**,** 759-762. doi: 10.1130/g34241.1.

Gottsmann, J., and Odbert, H. (2014). The effects of thermomechanical heterogeneities in island arc crust on time-dependent preeruptive stresses and the failure of an andesitic reservoir. *Journal of Geophysical Research: Solid Earth* 119**,** 4626-4639. doi: 10.1002/2014jb011079.

Gregg, P.M., De Silva, S.L., and Grosfils, E.B. (2013). Thermomechanics of shallow magma chamber pressurization: Implications for the assessment of ground deformation data at active volcanoes. *Earth and Planetary Science Letters* 384**,** 100-108. doi: 10.1016/j.epsl.2013.09.040.

Gregg, P.M., De Silva, S.L., Grosfils, E.B., and Parmigiani, J.P. (2012). Catastrophic caldera-forming eruptions: Thermomechanics and implications for eruption triggering and maximum caldera dimensions on Earth. *Journal of Volcanology and Geothermal Research* 241-242**,** 1-12. doi: 10.1016/j.jvolgeores.2012.06.009.

Gualda, G.a.R., Ghiorso, M.S., Lemons, R.V., and Carley, T.L. (2012). Rhyolite-MELTS: a Modified Calibration of MELTS Optimized for Silica-rich, Fluid-bearing Magmatic Systems. *Journal of Petrology*. doi: 10.1093/petrology/egr080.

Gudmundsson, A. (2006). How local stresses control magma-chamber ruptures, dyke injections, and eruptions in composite volcanoes *Earth-Science Reviews* 79**,** 1-31. doi: doi: 10.1016/j.earscirev.2006.06.006.

Gutiérrez, F., and Parada, M.A. (2010). Numerical Modeling of Time-dependent Fluid Dynamics and Differentiation of a Shallow Basaltic Magma Chamber. *Journal of Petrology* 51**,** 731-762. doi: 10.1093/petrology/egp101.

Holland, T., Baker, J., and Powell, R. (1998). Mixing properties and activity-composition and relationships of chlorites in the system MgO-FeO-Al 2 O 3 -SiO 2 -H 2 O. *European Journal of Mineralogy* 10**,** 395-406.

Holland, T., and Powell, R. (2003). Activity-composition relations for phases in petrological calculations: an asymmetric multicomponent formulation. *Contributions to Mineralogy and Petrology* 145**,** 492-501. doi: 10.1007/s00410-003-0464-z.

Holland, T.J.B., and Powell, R. (1998). An internally consistent thermodynamic data set for phases of petrological interest. *Journal of Metamorphic Geology* 16**,** 309-343. doi: 10.1111/j.1525-1314.1998.00140.x.

Jaeger, J.C. (1959). Temperatures outside a cooling intrusive sheet. *American Journal of Science* 257**,** 44-54. doi: 10.2475/ajs.257.1.44.

Jaeger, J.C. (1964). Thermal effects of intrusions. *Reviews of Geophysics* 2**,** 443-466. doi: 10.1029/RG002i003p00443.

Jaeger, J.C., Cook, N.G.W. and Zimmerman, R., 2007. Fundamentals of Rock Mechanics, 4th Edition. Wiley-Blackwell, 488 pp.

Jellinek, A., and De Paolo, D. (2003). A model for the origin of large silicic magma chambers:precursors of caldera -forming eruptions. *Bulletin of Volcanology* 65**,** 363-381.

Johnson, S.E., Jin, Z.-H., Naus-Thijssen, F.M.J., and Koons, P.O. (2011). Coupled deformation and metamorphism in the roof of a tabular midcrustal igneous complex. *Geological Society of America Bulletin*. doi: 10.1130/b30269.1.

Keller, T., May, D.A., and Kaus, B.J.P. (2013). Numerical modelling of magma dynamics coupled to tectonic deformation of lithosphere and crust. *Geophysical Journal International* 195**,** 1406-1442. doi: 10.1093/gji/ggt306.

Koyaguchi, T. and Kaneko, K., (2000). Thermal evolution of silicic magma chambers after basalt replenishments. *Geological Society of America Special Papers*, 350: 47-60. doi: 10.1130/0-8137-2350-7.47

Lovering, T.S. (1935). Theory of heat conduction applied to geological problems. *Geological Society of America Bulletin* 46**,** 69-94. doi: 10.1130/gsab-46-69.

Lovering, T.S. (1936). Heat Conduction in Dissimilar Rocks and the Use of Thermal Models. *Geological Society of America Bulletin* 47**,** 87-100. doi: 10.1130/gsab-47-87.

Lovering, T.S. (1955). Temperatures in and near intrusions. *Economic Geology* 50**,** 249-281.

Martí, J., Pinel, V., López, C., Geyer, A., Abella, R., Tárraga, M., Blanco, M.J., Castro, A., and Rodríguez, C. (2013). Causes and mechanisms of the 2011–2012 El Hierro (Canary Islands) submarine eruption. *Journal of Geophysical Research: Solid Earth* 118**,** 823-839. doi: 10.1002/jgrb.50087.

Miron, G., Wagner, T., Wälle, M., and Heinrich, C. (2013). Major and trace-element composition and pressure‚Äìtemperature evolution of rock-buffered fluids in low-grade accretionary-wedge metasediments, Central Alps. *Contributions to Mineralogy and Petrology* 165**,** 981-1008. doi: 10.1007/s00410-012-0844-3.

Nabelek, P.I., Hofmeister, A.M., and Whittington, A.G. (2012). The influence of temperature-dependent thermal diffusivity on the conductive cooling rates of plutons and temperature-time paths in contact aureoles. *Earth and Planetary Science Letters* 317‚Äì318**,** 157-164. doi: 10.1016/j.epsl.2011.11.009.

Peacock, S.M., and Spear, F.S. (2013). "Thermal Modeling of Metamorphic Pressure-Temperature-Time Paths: a Forward Approach," in *Metamorphic Pressure-Temperature-Time Paths*. American Geophysical Union), 57-102.

Petford, N., Cruden, A.R., McCaffrey, K.J.W. and Vigneresse, J.-L., (2000). Granite formation, transport and emplacement in the Earth's crust. *Nature*, 408: 669-673. doi: 10.1038/35047000

Petford, N.C.J.D., 2000. Granites are not diapiric! *Geology Today*, september-october,2000: 180-184. doi: 10.1111/j.1365-2451.2000.00008.x

Pla, F., and Álvarez-Valero, A.M. (2015). "Biot number constraints on the sub-volcanic crust magma thermal regime: an integrating approach of numerical modelling and petrology," in *Chemical, Physical and Temporal Evolution of Magmatic Systems*, eds. L. Caricchi & J.D. Blundy. Geological Society, London, Special Publications), 422.

Polat, A. (2009). The geochemistry of Neoarchean (ca. 2700 Ma) tholeiitic basalts, transitional to alkaline basalts, and gabbros, Wawa Subprovince, Canada: Implications for petrogenetic and geodynamic processes. *Precambrian Research* 168**,** 83-105. doi: 10.1016/j.precamres.2008.03.008.

Rodríguez, C., Geyer, A., Castro, A., and Villaseñor, A. (2015). Natural equivalents of thermal gradient experiments. *Journal of Volcanology and Geothermal Research* 298**,** 47-58. doi: 10.1016/j.jvolgeores.2015.03.021.

Rudnick, R.L., and Gao, S. (2003). "3.01 - Composition of the Continental Crust," in *Treatise on Geochemistry*, ed. H.D.H.K. Turekian. (Oxford: Pergamon), 1-64.

Sensarma, S., Hoernes, S., and Mukhopadhyay, D. (2004). Relative contributions of crust and mantle to the origin of the Bijli Rhyolite in a palaeoproterozoic bimodal volcanic sequance (Dongargarh Group), central India. *Proceedings of the Indian Academy of Science* 113**,** 619-648.

Turcotte, D.L. and Schubert, G., 2002. Geodynamics. Cambridge University Press, Cambridge, 456 pp. pp.

Tinkham, D.K., Zuluaga, C.A., and Stowell, H.H. (2001). Metapelitic phase equilibria modeling in MnNCKFMASH: the effect of variable Al2O3 and MgO/(MgO + FeO) on mineral stability. Geol. Mater. Res. 3, 1-42. *Geological Materials Research* 3**,** 1-42.

Wang, D. (2012). Comparable study on the effect of errors and uncertainties of heat transfer models on quantitative evaluation of thermal alteration in contact metamorphic aureoles: Thermophysical parameters, intrusion mechanism, pore-water volatilization and mathematical equations. *International Journal of Coal Geology* 95**,** 12-19. doi: 10.1016/j.coal.2012.02.002.

Wang, D., Song, Y., Liu, Y., Zhao, M., Qi, T., and Liu, W. (2012). The influence of igneous intrusions on the peak temperatures of host rocks: Finite-time emplacement, evaporation, dehydration, and decarbonation. *Computers & Geosciences* 38**,** 99-106. doi: 10.1016/j.cageo.2011.05.011.

Whittington, A.G., Hofmeister, A.M. and Nabelek, P.I. (2009). Temperature-dependent thermal diffusivity of the Earth/'s crust and implications for magmatism. *Nature*, 458(7236): 319-321. doi: 10.1038/nature07818

Yogodzinski, G.M., Volynets, O.N., Koloskov, A.V., Seliverstov, N.I., and Matvenkov, V.V. (1994). Magnesian Andesites and the Subduction Component in a Strongly Calc-Alkaline Series at Piip Volcano, Far Western Aleutians. *Journal of Petrology* 35**,** 163-204. doi: 10.1093/petrology/35.1.163.

Graphical abstract

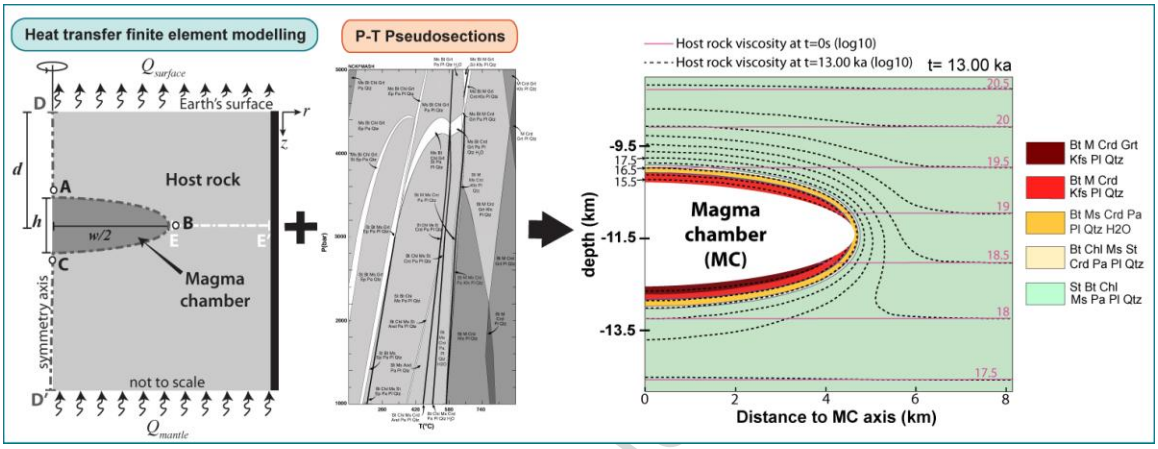

Modeling magmatic intrusions of different compositions and geometries in the upper crust: Implications for the thermomechanical behavior of the country rocks

Madison M. Douglas[1], Adelina Geyer[2], Antonio M. Álvarez-Valero[3], Joan Martí[2]

Highlights

- Host rocks suffer petrological and thermomechanical effects due to magma intrusion
- We numerically model conductive cooling of a magma chamber within the upper crust
- Temperature field is integrated with metamorphic effects through phase diagrams
- Reservoir geometry plays a dominant role in controlling the effects on the host rock
- Results may be used in further studies of magma chamber stability and integrity